Control and Cybernetics
vol. 54 (2025) No. 3
pages: 259-288
DOI: 10.2478/candc-2025-0009

Optimal block-mode assignment and relocation in matrix polynomials for observer-based static and dynamic multivariable feedback compensators*

by

Kamel Kadri[1], **Farès Boudjema**[2], **Bachir Nail**[3] **and Imad Eddine Tibermacine**[4]

[1]Complex Systems Control and Simulators (CSCS) Laboratory,
Ecole Militaire Polytechnique, Bordj el Bahri 16046, Algiers, Algeria
[2]Process Control Laboratory, Control Engineering Department,
National Polytechnic School (ENP), 10, Av. Hassen Badi, BP. 182, Algiers, Algeria
[3]Renewable Energy Systems Applications Laboratory (LASER),
Faculty of Sciences and Technology, Ziane Achour University, Djelfa, Algeria
[4]Department of Computer, Automation and Management Engineering,
Sapienza University of Rome, Rome, Italy
Corresponding author (Bachir Nail): nail_bachir@yahoo.fr

Abstract: This study introduces an observer-based dual strategy for optimizing block mode placement in matrix polynomial control systems, focusing on improving stability and performance in multivariable feedback applications. It introduces two approaches: a static state feedback compensator for a challenging Bidirectional Inductive Power Transfer (IPT) System, and a dynamic observer-based output feedback compensator for a defensive air-to-surface missile control problem. Both designs exploit the Grey Wolf Optimizer to solve the nonlinear convex optimization, associated with block mode selection. The dynamic plan employs Luenberger observer principles for unmeasured state estimation, ensuring system reliability through strict observability conditions. Simulation results reveal that the proposed optimal placement methods enhance tracking, boost stability margins, and substantially minimize control effort. Overall, this methodology offers an effective framework for robust controller design and state estimation across disparate, complex dynamic systems, while reducing computational burden and improving control efficiency.

Keywords: block modes, matrix polynomials, static compensator algorithm, dynamic observer-based compensator, multivariable systems, bidirectional IPT System, Grey Wolf Optimizer

*Submitted: November 2022; Accepted: October 2025

1. Introduction

Matrix polynomial theory has evolved as a cornerstone mathematical framework within contemporary multivariable control system design, demonstrating exceptional capability in both state and observer-based output feedback configurations. The fundamental strength of matrix polynomials resides in their inherent capacity to simultaneously manipulate block-roots, containing latent eigenvalues, and block-vectors, encompassing corresponding eigenvectors, a distinctive feature unavailable in conventional scalar-based methodologies, see Nail, Kouzou and Hafaifa (2019).

Block-mode matrices embody the mathematical essence of matrix polynomial theory, wherein block-roots R encapsulate system eigenvalue information, while block-vectors r dictate response characteristics. This concurrent assignment capability provides unprecedented design flexibility in feedback compensator synthesis, enabling strategic placement on either system configuration with controllable, diagonal, or observable canonical forms to optimize performance, see Yaici and Hariche (2014).

Observer-based control systems have emerged as fundamental paradigms in modern control theory, particularly when complete state information is unavailable over direct measurement. The integration of state observers with block-mode assignment techniques creates a powerful framework for multivariable system control, enabling simultaneous state estimation and optimal controller synthesis, see Trentelman and Antsaklis (2015).

Contemporary research demonstrates increasing integration of comprehensive matrix polynomial block-mode collections into diverse multivariable control theoretical developments and practical implementations. Block-mode utilization enhances closed-loop system robustness against perturbations, while maintaining reduced sensitivity characteristics through expanded design freedom, compared to traditional scalar root assignment approaches, see Bekhiti et al. (2015).

One of the more recent areas of research concerns the incorporation of the whole set of matrix polynomial block modes into various multivariate control system theoretical developments and their respective implementations. Using the block modes provides the CLS with a low sensitivity and a significant robustness toward the perturbations. This is because, in places where it would normally assign the scalar roots, provides, instead, a significant degree of freedom. There are a variety of research publications that center their attention on state-feedback controllers, which suggest answers to issues of instability. In this stream of work we find: state-feedback stabilizer and integral-robust adaptive state-feedback control applied to some uncertain and switched LTI systems (Tanaka and Langbert, 2011; Xiang, Xiao and Jiang, 2015), a state-feedback designed via a realization of a complete column rank compensators (Castañeda-Toledo, Kučera and Ruiz-Léon, 2015; Gkizas et al., 2018; Yang et al., 2018; Yaici and Hariche, 2014).

The present study advances matrix polynomial theory by enhancing its properties through systematic block-mode optimization, utilizing state-of-the-art swarm intelligence algorithms, and most notably, the Grey Wolf Optimizer framework (Nail, Kouzou and Hafaifa, 2019). This study adopts a dual methodological approach, comprising static state feedback compensator synthesis to address systems with intrinsic controllability deficiencies and dynamic observer-based output feedback compensator development, tailored for complex guidance and tracking scenarios. For the static controller, optimal positioning strategies for feedback matrix parameters K are determined to achieve robust closed-loop performance, with the Bidirectional Inductive Power Transfer system serving as an exemplary case study. The inherent structural limitations of the IPT system's controllability matrix require advanced optimization strategies to rigorously identify advantageous block-mode configurations.

Internal stability considerations remain paramount within control theory, as industrial systems demand unwavering stability to mitigate substantial operational risks and economic losses, a reality underscored in critical sectors such as aerospace propulsion, nuclear energy, and chemical processing. To benchmark dynamic controller designs, the study explores the formulation of dynamic compensators through Left Matrix Fraction Description, subsequently transforming system models to Right Matrix Fraction Description form. The autopilot-guided missile system, characterized by highly nonlinear dynamics with swiftly varying uncertainties, is employed as a challenging application to validate dynamic compensator efficacy. To comprehensively assess methodological excellence and algorithmic resilience, extensive comparative analyses are conducted between the established Grey Wolf Optimizer and some other contemporary metaheuristic algorithms, thereby establishing the superiority and robustness of the proposed optimization-driven control strategies across diverse application domains.

2. Matrix polynomial theoretical foundation

2.1. Preliminaries

Matrix polynomial theory provides the fundamental mathematical framework for the proposed observer-based dual control methodology. Consider the multivariable LTI system representation:

$$\begin{cases} \dot{\xi}_t = A\xi_t + B\mu_t \\ \mathcal{Y}_t = C\xi_t + D\mu_t \end{cases}, \tag{1}$$

where $\xi \in \mathbb{R}^n$ represents the state space vector, $A \in \mathbb{R}^{n\times n}$ denotes the system matrix, $B \in \mathbb{R}^{n\times m}$ constitutes the input matrix, $C \in \mathbb{R}^{p\times n}$ represents the output matrix, and $D \in \mathbb{R}^{p\times m}$ defines the coupling matrix.

The controllability subspace χ_c is generated by vectors $A^i B$ as:

$$\chi_c = \text{span}\left\{A^i B\right\}_{i=0}^{l-1} \Longleftrightarrow \Omega_c = \text{row}\left(A^i B\right)_{i=0}^{l-1}, \tag{2}$$

where Ω_c represents the block controllability matrix.

Observability foundation:

The observability subspace χ_o is constructed from vectors CA^i:

$$\chi_o = \text{span}\left\{CA^i\right\}_{i=0}^{l-1} \Longleftrightarrow \Omega_o = \text{col}\left(CA^i\right)_{i=0}^{l-1}. \tag{3}$$

Observability matrix:

The observability matrix for system (1) is defined as:

$$\mathcal{O}_n = \begin{bmatrix} C \\ CA \\ CA^2 \\ \vdots \\ CA^{n-1} \end{bmatrix} \in \mathbb{R}^{np\times n}. \tag{4}$$

DEFINITION 1 ***Observability condition:*** *The system (1) is observable if and only if the observability matrix $\mathcal{O}_n$ has full column rank, i.e., rank($\mathcal{O}_n$) = n.*

The controllable canonical transformation produces:

$$\begin{cases} \dot{\xi}_{c(t)} = \left\{A_c = T_c A {T_c}^{-1}\right\} \xi_{ct} + \{B_c = T_c B\} \mu_t \\ \mathcal{Y}_t = \left\{C_c = C{T_c}^{-1}\right\} \xi_{ct} + \{D_c = D\} \mu_t \end{cases} \tag{5}$$

with transformation matrices:

$$\begin{cases} T_c = \text{col}\left\{T_{c1} A^i\right\}_{i=0}^{l-1} \\ T_{c1} = B_c^T \left(\text{row}\left(A^i B\right)_{i=0}^{l-1}\right)^{-1}. \end{cases} \tag{6}$$

Observable canonical form:

Similarly, the observable canonical transformation yields:

$$\begin{cases} \dot{\xi}_o(t) = \left\{A_o = T_o^{-1} A T_o\right\} \xi_{ot} + \left\{B_o = T_o^{-1} B\right\} \mu_t \\ \mathcal{Y}_t = \{C_o = C T_o\} \xi_{ot} + \{D_o = D\} \mu_t \end{cases} \tag{7}$$

where:

$$\begin{cases} T_o = \text{row}\left\{A^i T_{o1}\right\}_{i=0}^{l-1} \\ T_{o1} = \left(\text{col}\left\{CA^i\right\}_{i=0}^{l-1}\right)^{-1} C_o^T. \end{cases} \tag{8}$$

The matrices denoted by the symbols Im, Ip and Om, Op, respectively, are the identity matrix and the zero matrix, while the symbol T signifies the transpose.

μ_t is the variable vector that is being forced, and $\mathscr{Y}_t$ is the variable vector that is being output (measurement function).

The controllability state variable vector is denoted by ξ_{ct}, while the observability is denoted by ξ_{ot}.

The notation **row** refers to the block row operator, **col** refers to the block column operator, and **span** refers to the construction of the maximum linearly independent vectors.

REMARK 1 *Block canonical transformations are feasible for system (1) into both controllable and observable forms when rank of* $\{\Omega_c, \Omega_o\} = n$, *and the ratio* $\{n/m, n/p\} = l$ *is integer. For observer-based control, observability is crucial as it ensures the feasibility of state estimation.*

2.2. Block-modes conceptualization in matrix polynomials

Block-modes $R \in \mathbb{R}^{m\times m}$ of polynomial matrix $A(s)$ constitute the primary design focus for right-side system placement, see Yaici and Hariche (2014). Consider a polynomial matrix of order m and degree l:

$$D_r(s) = I_m s^l + A_1 s^{l-1} + \ldots + A_l. \tag{9}$$

Right block-modes are defined by matrices $R \in \mathbb{R}^{m\times m}$, satisfying:

$$D_r(R) = A_0 R^l + A_1 R^{l-1} + \ldots + A_{l-1} R + A_l = 0_m. \tag{10}$$

The selected block-modes $R \in \mathbb{R}^{m\times m}$ derive from dominant stable latent eigenvalues. Multiple configurations can be chosen without compromising closed-loop dynamics. The diagonal form provides excellent controller design performance (Yaici and Hariche, 2014; Nail, Kouzou and Hafaifa, 2019):

$$R = \mathrm{diag}(R_1, R_2, \ldots, R_l), \tag{11}$$

where each R_i contains appropriately selected eigenvalues for desired closed-loop characteristics.

$$R = \left(\overbrace{\underbrace{r_1 \left(\begin{array}{c|c|c} \lambda_1 & 0 & 0 \\ \hline 0 & \ddots & 0 \\ \hline 0 & 0 & \lambda_m \end{array}\right) r_1^{-1}}_{R_1}, \ldots, \underbrace{r_l \left(\begin{array}{c|c|c} \lambda_{n-m+1} & 0 & 0 \\ \hline 0 & \ddots & 0 \\ \hline 0 & 0 & \lambda_n \end{array}\right) r_l^{-1}}_{R_l}}^{\lambda_{\overline{1,\ldots,n}}} \right). \tag{12}$$

2.3. The verification of complete set condition

$\{R_1, R_2, \ldots, R_l\}$ is considered as a set of block-modes, designed on the basis of the following eigenvalues $(\lambda_1, \lambda_2, \ldots, \lambda_n)$ of the block controller form matrix A_c, where $\{R_1, R_2, \ldots, R_l\}$ is a complete set of block-modes if (see Yaici and Hariche, 2014; Bekhiti et al., 2018):

$$\begin{cases} \sigma(R_i) \cup \sigma\left(R_j\right) = \sigma(A_c) \\ \sigma(R_i) \cap \left(R_j\right) = \emptyset \\ \det\left(V_r\left(R_1, R_2, \ \ldots\ , R_l\right)\right) \neq 0 \end{cases} . \tag{13}$$

where σ is the spectrum of the matrix, V_r is the right block Vandermonde matrix, corresponding to $\{R_1, R_2, \ldots, R_l\}$, given as:

$$V_r\left(R_1, R, \ldots, R_l\right) = \begin{pmatrix} I_m & I_m & \cdots & I_m \\ R_1 & R_2 & \cdots & R_l \\ \vdots & \vdots & \ddots & \vdots \\ {R_1}^{l-1} & {R_2}^{l-1} & \cdots & {R_l}^{l-1} \end{pmatrix}. \tag{14}$$

REMARK 2 *The right block Vandermonde matrix V_r must be nonsingular.*

3. Problem statement

3.1. Static compensator

The static compensator design objective involves applying negative state feedback control $u = -Kx(t)$ to system (1), where $K \in \mathbb{R}^{m\times n}$. Through optimization-based block transformation to controller form, right diagonal block-modes are assigned using the right Vandermonde matrix. The goal is to determine the minimum norm feedback matrix gain K, preserving global closed-loop stability, as depicted in Fig. 2.

The optimization problem consists in:

$$\min_K \|K\|_\infty \quad \text{subject to} \quad \mathrm{Re}(\lambda(A - BK)) < 0. \tag{15}$$

3.2. Dynamic observer-based compensator

Observer design theory integration:

The dynamic compensator synthesis employs a comprehensive observer-based approach integrating Left Matrix Fraction Description (LMFD) design methodology

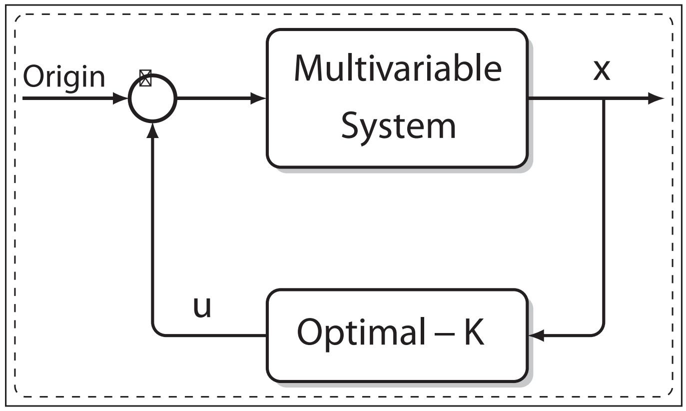

Figure 1: Static state feedback stabilization scheme

with Luenberger observer principles. The system transforms to Right Matrix Fraction Description (RMFD) through algebraic manipulations, while simultaneously designing a state observer for unmeasured states.

State estimation framework:

Consider the system (1), where only the output $y(t) = Cx(t)$ is measurable. A Luenberger observer is designed to estimate the unmeasured states $\hat{x}(t)$ using:

$$\dot{\hat{x}}(t) = A\hat{x}(t) + Bu(t) + L(y(t) - C\hat{x}(t)) \tag{16}$$

where $L \in \mathbb{R}^{n\times p}$ is the observer gain matrix, designed to ensure estimation error convergence.

Estimation error dynamics:

The estimation error $e(t) = x(t) - \hat{x}(t)$ evolves according to:

$$\dot{e}(t) = (A - LC)e(t). \tag{17}$$

Observer stability condition:

The observer is stable if and only if all eigenvalues of $(A - LC)$ have negative real parts, i.e., $\mathrm{Re}(\lambda_i(A - LC)) < 0$ for all i.

Observability conditions for observer design:

The observer gain L can be designed if and only if the pair (A, C) is observable.

This is equivalent to the observability condition:

$$\operatorname{rank}\left(\begin{bmatrix} C \\ CA \\ CA^2 \\ \vdots \\ CA^{n-1} \end{bmatrix}\right) = n. \tag{18}$$

Observer-based control architecture:

The complete observer-based compensator structure follows:

$$\begin{cases} \dot{\hat{x}}(t) = A\hat{x}(t) + Bu(t) + L(y(t) - C\hat{x}(t)) & \text{(state observer)} \\ u(t) = -K\hat{x}(t) + N_c r(t) & \text{(control law)} \end{cases} \tag{19}$$

where $r(t)$ is the reference signal and N_c is the reference tracking gain.

The compensator structure follows the transfer function representation:

$$H_c(s) = D_c(s)^{-1} N_c(s) \tag{20}$$

where optimal coefficient matrices are determined through block-mode optimization techniques, integrated with observer pole placement.

Separation principle application:

The observer-based design leverages the separation principle, allowing independent design of the state feedback controller and the state observer, provided both controllability and observability conditions are satisfied (Nail et al., 2018).

4. Methods

4.1. Static compensator algorithm

Following block controller form transformation T_c application, system (1) converts to block controller form (5). The resulting state feedback control becomes equal $u = -K_c x_c(t)$, where $K_c \in \mathbb{R}^{m\times n}$ and:

$$K = K_c T_c = \left(K_{cl}, K_{c(l-1)}, \ldots, K_{c1}\right) T_c \tag{21}$$

with $K_{ci} \in \mathbb{R}^{m\times m}$ for $i = 1, \ldots, l$.

The closed-loop system expression becomes:

$$\begin{cases} \dot{x}_c(t) = (A_c - B_c K_c)\, x_c(t) \\ y_c(t) = C_c x_c(t) \end{cases} \tag{22}$$

where

$$(A_c - B_c K_c) = \begin{pmatrix} O_m & \cdots & O_m \\ O_m & \cdots & O_m \\ \vdots & \ldots & \vdots \\ O_m & \cdots & I_m \\ -(A_l + K_{cl}) & \cdots & -(A_1 + K_{c1}) \end{pmatrix}. \tag{23}$$

The characteristic matrix polynomial of the closed-loop system takes the form:

$$D_r(s) = I_m s^l + (A_1 + K_{c1}) s^{l-1} + \ldots + (A_l + K_{cl}). \tag{24}$$

From n selected eigenvalues, the optimal complete set of l block-modes are designed diagonally:

$$R(\mathbf{x}) = \operatorname{diag}(R_1(\mathbf{x}), R_2(\mathbf{x}), \ldots, R_l(\mathbf{x})) \tag{25}$$

$$R(\mathbf{x}) = \left(\overbrace{\underbrace{r_1 \left(\begin{array}{c|c|c} \mathbf{x}_1 & 0 & 0 \\ \hline 0 & \ddots & 0 \\ \hline 0 & 0 & \mathbf{x}_m \end{array} \right) r_1^{-1}}_{R_1(\mathbf{x})}, \ldots, \underbrace{r_l \left(\begin{array}{c|c|c} \mathbf{x}_{n-m+1} & 0 & 0 \\ \hline 0 & \ddots & 0 \\ \hline 0 & 0 & \mathbf{x}_n \end{array} \right) r_l^{-1}}_{R_l(\mathbf{x})}}^{\mathbf{x}_{\overline{1,\ldots,n}}} \right). \tag{26}$$

The right block Vandermonde matrix, corresponding to $\{R_1(\mathbf{x}), R_2(\mathbf{x}), \ldots, R_l(\mathbf{x})\}$, is:

$$V_r(\mathbf{x}) = \begin{pmatrix} I_m & I_m & \cdots & I_m \\ R_1(\mathbf{x}) & R_2(\mathbf{x}) & \cdots & R_l(\mathbf{x}) \\ \vdots & \vdots & \ddots & \vdots \\ R_1(\mathbf{x})^{l-1} & R_2(\mathbf{x})^{l-1} & \cdots & R_l(\mathbf{x})^{l-1} \end{pmatrix}. \tag{27}$$

The desired characteristic matrix polynomial is expressed as:

$$D_d(\mathbf{x}) = -\left[R_1(\mathbf{x})^{l-1}, R_2(\mathbf{x})^{l-1}, \ldots, R_l(\mathbf{x})^{l-1} \right] V_r(\mathbf{x})^{-1}. \tag{28}$$

By equating (28) = (24) $\Rightarrow D_d(\mathbf{x}) = D_r(s)$, we obtain:

$$K_c(\mathbf{x}) = \left[D_d(\mathbf{x})^T + A_c((n-m+1):n,:)^T \right]^T. \tag{29}$$

A nonlinear matrix function is denoted by the symbol $K_c(\mathbf{x})$. In order to acquire the best matrix gain that will lead to the desired closed-loop stability system, equation (????) is evolved into a problem of convex optimization by the addition of constraints. This allows for the best possible chance of obtaining the desired result.

The metaheuristics constraints optimization tool GWO (Mirjalili, Mirjalili and Lewis, 2014) is able to rectify this issue, and the proposed objective function $f(\mathbf{x})$ can be written as follows:

$$f(\mathbf{x}) = \|K_c(\mathbf{x})\|_\infty . \tag{30}$$

Now, the problem is to find $\mathbf{x}$, which minimizes the objective function $\min_{\mathbf{x}} f(\mathbf{x})$ subject to a certain set of constraints:

$$\left| \begin{array}{l} \operatorname{Re}(\lambda(A_c - B_c K_c)) < 0 \\ V_r V_r^{-1} - I_n = 0 \\ lb \le \mathbf{x} \le ub, \qquad \{lb, ub\} \in]-\infty \;\; +\infty[-\{0\} \end{array} \right. . \tag{31}$$

When it comes to the CLS, the function of the inequality constraint condition is to serve as a regulator for the stability convergence. This is accomplished by the application of the inequality constraint condition. In order to ensure the existence of the correct block-Vandermonde matrix V_r, equality constraints are utilized. This is required due to the fact that the inverse of the matrix creates challenges when it comes to the process of creating the controller (ill-conditioned matrix and system). The lower and upper bounds of the optimization vector $\mathbf{x} \in R^n$ present the hidden eigenvalues of the matrix. The reason for this is that the values of this vector map onto the left side of the s-plane. Not to mention [????] the fact that the gain of the static state feedback matrix, denoted by K, is represented in the fundamental space as follows:

$$K = K_c T_c . \tag{32}$$

4.2. Dynamic observer-based compensator algorithm

Observer-based design integration:

The dynamic compensator algorithm incorporates observer design principles through the following comprehensive framework:

Step 1: Observability verification Verify that the system satisfies the observability condition by checking:

$$\operatorname{rank}(\mathcal{O}_n) = \operatorname{rank} \begin{bmatrix} C \\ CA \\ \vdots \\ CA^{n-1} \end{bmatrix} = n. \tag{33}$$

Step 2: Observer gain design Design the observer gain matrix L using pole placement technique to achieve the desired observer eigenvalues $\{\lambda_{o1}, \lambda_{o2}, \ldots, \lambda_{on}\}$:

$$L = \operatorname{place}(A^T, C^T, [\lambda_{o1}, \lambda_{o2}, \ldots, \lambda_{on}])^T . \tag{34}$$

Step 3: RMFD transformation with observer integration The system transforms to RMFD form through algebraic block transformations while incorporating observer dynamics:

$$[D_s] = (W_c)^{-1}\Gamma \quad \text{and} \quad [N_s] = W_c\Pi. \tag{35}$$

The resulting right matrix transfer function becomes:

$$H(s) = N(s)D^{-1}(s) = \left(\sum_{i=0}^{1} N_i s^i\right)\left(\sum_{i=0}^{2} D_i s^i\right)^{-1}. \tag{36}$$

Step 4: Observer-based compensator structure The proposed observer-based compensator integrates state estimation with control synthesis:

$$H_c(s) = D_c(s)^{-1}N_c(s) = \left(\sum_{i=0}^{2} D_{ci} s^i\right)^{-1}\left(\sum_{i=0}^{2} N_{ci} s^i\right), \tag{37}$$

where the coefficients D_{ci} and N_{ci} are optimized considering both control performance and observer dynamics.

Step 5: Observer-controller separation The complete observer-based compensator dynamics are given by:

$$\begin{cases} \dot{\xi}_c(t) = (A_c - B_cK_c - L_cC_c)\xi_c(t) + B_c u_r(t) + L_c y(t) \\ u(t) = K_c\xi_c(t) + N_c u_r(t) \end{cases} \tag{38}$$

where $\xi_c(t)$ represents the observer state, $u_r(t)$ is the reference input, and L_c is the observer gain in canonical form.

The closed-loop matrix transfer function for unity feedback configuration is given by:

$$H_{cl} = N(s)(D_c(s)D(s) + N_c(s)N(s))^{-1}N_c(s). \tag{39}$$

Observer-controller optimization:

The optimization constructs optimal compensator $\{D_c(s), N_c(s)\}$ by forcing matrix polynomial $D_f(s) = D_c(s)D(s) + N_c(s)N(s)$ to achieve the desired behavior using nonlinear optimization, while ensuring that the observer pole placement satisfies:

$$\mathrm{Re}(\lambda_i(A - LC)) < -\alpha, \quad \alpha > 0, \quad \forall i. \tag{40}$$

The optimal block root set derives from constraint target eigenvalues with diagonal design similar to the static case, but now incorporates observer dynamics constraints.

5. Numerical applications

5.1. Grey Wolf optimization algorithm

The GWO technique represents a contemporary metaheuristic approach, introduced by Mirjalili, Mirjalili and Lewis (2014). This nature-inspired computational method draws inspiration from the collective hunting strategies, exhibited by wolf packs in their natural habitat. The algorithm operates through a hierarchical structure that categorizes the wolf population into four distinct tiers: alpha (α), beta (β), delta (δ), and omega (ω). The optimization process relies on the three dominant wolves (α, β, and δ) to direct the subordinate members (ω) throughout the exploration phase toward optimal solutions (see Han, 2021).

5.1.1. Leadership hierarchy

In the GWO framework, the search space is organized according to wolf pack dominance structures. The most promising solution candidate is designated as the alpha (α) wolf, representing the leadership position. Subsequently, the beta (β) and delta (δ) wolves correspond to the second and third most favorable solutions in the search space. All remaining solution candidates are classified as omega (ω) wolves. Throughout the optimization process, the alpha wolf leads the search effort, supported by beta and delta wolves in decision-making roles. Consequently, the omega wolves adjust their search positions by following the guidance provided by these three superior individuals.

5.1.2. Prey encirclement mechanism

The mathematical representation of the encirclement behavior during the hunting process is expressed through the following equations:

$$\vec{D} = |\vec{C}\vec{X}_p(t) - X(t)| \tag{41}$$

$$\vec{X}(t+1) = |\vec{X}_p - \vec{A}\vec{D}| \tag{42}$$

where t denotes the iteration number; $\vec{A}$ and $\vec{C}$ are coefficient vectors; D represents the distance separating the wolf from its target; $\vec{X}_p$ indicates the prey's position vector; and $\vec{X}$ signifies the wolf's current position vector.

The coefficient vectors $\vec{A}$ and $\vec{C}$ are determined using:

$$\vec{A} = 2\vec{a}\vec{r}_1 - \vec{a} \tag{43}$$

$$\vec{C} = 2\vec{r}_2 \tag{44}$$

where $\vec{a}$ undergoes linear reduction from 2 to 0 across iterations, while $\vec{r}_1$ and $\vec{r}_2$ represent random vectors, uniformly distributed within the interval [0,1].

5.1.3. Hunting strategy

Grey wolves possess the ability to detect prey locations and perform coordinated encirclement maneuvers. The alpha wolf primarily orchestrates the hunting sequence, with beta and delta wolves occasionally contributing to the pursuit strategy. Nevertheless, determining the precise location of the global optimum (analogous to prey) within an abstract optimization landscape remains uncertain. To address this challenge, the algorithm assumes that the alpha (representing the optimal solution), beta, and delta wolves possess superior knowledge regarding promising search regions. Accordingly, the three best solutions identified at each iteration are retained, while omega wolves modify their positions relative to these elite agents. This positioning strategy is formalized through the following mathematical expressions:

$$\begin{cases} \vec{D}_\alpha = |\vec{C}_1 \vec{X}_\alpha - \vec{X}| \\ \vec{D}_\beta = |\vec{C}_2 \vec{X}_\beta - \vec{X}| \\ \vec{D}_\delta = |\vec{C}_3 \vec{X}_\delta - \vec{X}| \end{cases} \tag{45}$$

$$\vec{X}_1 = |\vec{X}_\alpha - \vec{A}_1 (D_\alpha)| \tag{46}$$

$$\vec{X}_2 = |\vec{X}_\beta - \vec{A}_2 (D_\beta)| \tag{47}$$

$$\vec{X}_3 = |\vec{X}_\delta - \vec{A}_3 (D_\delta)| \tag{48}$$

$$\vec{X}(t+1) = \frac{\vec{X}_1 + \vec{X}_2 + \vec{X}_3}{3}. \tag{49}$$

In these equations, $\vec{X}_\alpha$, $\vec{X}_\beta$, and $\vec{X}_\delta$ denote the spatial coordinates of the alpha, beta, and delta wolves, respectively. The vectors $\vec{C}_1$, $\vec{C}_2$, and $\vec{C}_3$ are stochastic coefficients, computed according to equations (43) and (44), while $\vec{X}$ represents the position of the solution being updated.

5.1.4. Comparison of algorithms

In a direct comparison of closed-loop performance and energy efficiency, the GWO algorithm demonstrated either superior or equally robust results against the background of the techniques ranging from the most recent Particle Swarm Optimization (PSO), Genetic Algorithm (GA), Differential Evolution (DE), down to Harris Hawk Optimization (HHO) methods, according to recent benchmarks, Saheed, Omole and

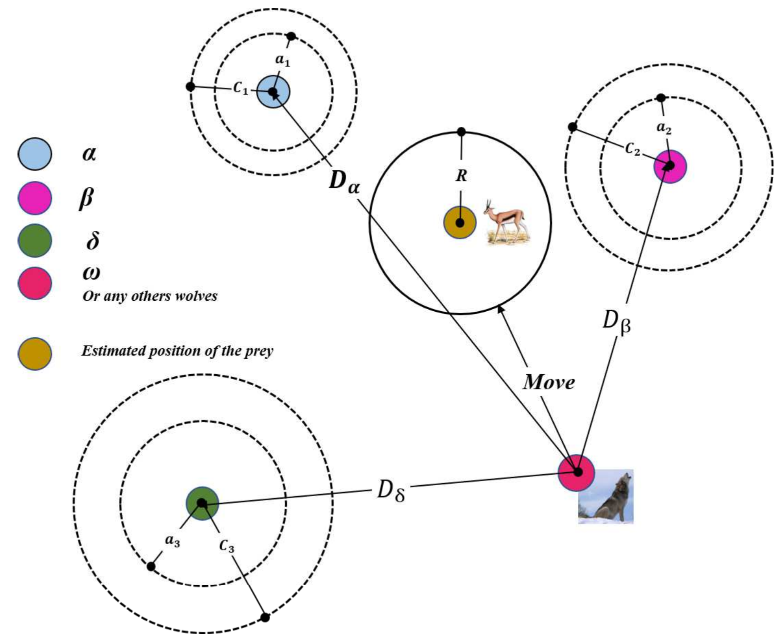

Figure 2: Position update in GWO

Sabit (2025), Ren and Meng (2025), Wang and Wei (2025). GWO's hierarchical search process is especially effective for matrix polynomial root assignment problems, explaining its selection for both static and dynamic compensator design in this work.

Table 1: Comparative performance of optimization algorithms.

Criterion	GWO	PSO	GA	DE	HHO
Stability	High	High	Moderate	High	High
Convergence	Fast	Fast	Moderate	Faster	Fast
Energy usage	Low	Moderate	Moderate	Low	Moderate
Robustness	Strong	Good	Good	Strong	Good
Reference	A	B	C	D	E

References: A: Kadiri et al. (2023a); B: Kadiri et al. (2023b); C: Saheed, Omole and Sabit (2015); D: Ren and Meng (2025); E: Wang and Wei (2025)

5.2. Static compensator

We performed the suggested controller algorithm steps on the IPT system in the following manner in order to accomplish the primary objectives of this paper:

- $l = n/m = 8/2 = 4$. The system can be transformed in blocks.
- Rank $(\Omega) = 8$ indicates that block controllability has been verified (is a completely state full rank block controllable).
- The matrix of transformations for the block controller, $T_c \in R^{8\times 8}$, is computed.

Problem In spite of this, the block controllability matrix Ω_c has a rank that is complete. The fact that the determinant of Ω_c is quite close to zero, as shown by the expression $\det(\Omega) = -1.39 \times 10^{-22}$, indicates that the controllability of the system is poor and that a specific solution, based on optimization techniques, is required to address the issue.

- $l = 4$, which means that the four desired block-modes $\{R_1(\mathbf{x}), R_2(\mathbf{x}), R_3(\mathbf{x}), R_4(\mathbf{x})\} \in R^{2\times 2}$ are assigned and chosen diagonally (14) in the following manner:

$$\left(\overbrace{\underbrace{r_1\left(\begin{array}{c|c}\mathbf{x}_1 & 0\\ \hline 0 & \mathbf{x}_2\end{array}\right)r_1^{-1}}_{R_1(\mathbf{x})}, \underbrace{r_2\left(\begin{array}{c|c}\mathbf{x}_3 & 0\\ \hline 0 & \mathbf{x}_4\end{array}\right)r_2^{-1}}_{R_2(\mathbf{x})}, \underbrace{r_3\left(\begin{array}{c|c}\mathbf{x}_5 & 0\\ \hline 0 & \mathbf{x}_6\end{array}\right)r_3^{-1}}_{R_3(\mathbf{x})}, \underbrace{r_4\left(\begin{array}{c|c}\mathbf{x}_7 & 0\\ \hline 0 & \mathbf{x}_8\end{array}\right)r_4^{-1}}_{R_4(\mathbf{x})}}^{\mathbf{x}_{\overline{1,\dots,8}}}\right).$$

- Given this, the following is the right block Vandermonde matrix $V_r(\mathbf{x}) \in R^{8\times 8}$:

$$V_r(\mathbf{x}) = \begin{pmatrix} I_2 & I_2 & \cdots & I_2\\ R_1(\mathbf{x}) & R_2(\mathbf{x}) & \cdots & R_4(\mathbf{x})\\ \vdots & \vdots & \ddots & \vdots\\ R_1(\mathbf{x})^3 & R_2(\mathbf{x})^3 & \cdots & R_4(\mathbf{x})^3 \end{pmatrix}.$$

- The appropriate characteristic matrix polynomial can be designed by utilizing (16), which is based on a collection of block-modes:

$$D_d(\mathbf{x}) = -\left[R_1(\mathbf{x}), R_2(\mathbf{x}), R_3(\mathbf{x}), R_4(\mathbf{x})\right] V_r(\mathbf{x})^{-1}.$$

- From (17), $K_c(\mathbf{x})$ is obtained as follows:

$$K_c(\mathbf{x}) = \left[D_d(\mathbf{x})^T + Ac(\overline{7:8},:)^T\right]^T.$$

And,

$$Ac(\overline{7:8},\ :)^T = \begin{pmatrix} -0.0002 & 0.0001\\ 0.0001 & -0.0002\\ -0.0000 & 0.0000\\ 0.0000 & -0.0000\\ -0.0371 & 0.0068\\ 0.0069 & -0.0368\\ -0.0011 & 0.0003\\ 0.0003 & -0.0011 \end{pmatrix}.$$

- The GWO optimization tool is utilized to solve this problem so that the optimal $Kc(\mathbf{x})$ may be computed. This $Kc(\mathbf{x})$ will reach the minimal feasible norm matrix gains while also meeting the CLS stability conditions in an effective manner. 'The obtained vector $\mathbf{x}$ that minimizes $\min \mathbf{x} \| Kc(\mathbf{x}) \| \infty$ is checked as follows:

  1. $\mathrm{Re}\,(\lambda(A_c - B_c K_c)) < 0,$ checked by definition.
  2. $V_r V_r^{-1} = I_8,$ checked.
  3. $-4 \leq \mathbf{x} \leq 4,$ checked.

Following the resolution of the optimization issue that was handled by the GWO optimizer, the following values are assigned to the optimizer's parameters: the optimization vector $\mathbf{x} \in \mathbb{R}^{24}$, where the lower bound and the upper bound vectors are given as:

$$lb = [-4 * \mathrm{ones}(1,8) \ \ -4 * \mathrm{ones}(1,16)] \text{ and } ub = [-0.01 * \mathrm{ones}(1,8) \ \ 4 * \mathrm{ones}(1,16)],$$

respectively, where this vector's first interval corresponds to the eigenvalues space, while this vector's second interval corresponds to the eigenvectors space, respectively. This remarkable benefit makes it possible to assign both the eigenvalues and the eigenvectors at the same time. The number of search agents is set to 20, and the number of iterations is set to 500, as can be seen in the figures, which follow. A flowchart that provides a summary of all the stages involved in the suggested methods is shown in Fig. 4.

The optimal eigenvalues vector obtained using GWO is the following one:

$$\lambda = \begin{pmatrix} \lambda & \lambda^* \\ -0.0100 + 0.1843\mathrm{i} & -0.0100 - 0.1843\mathrm{i} \\ -0.0100 + 0.1567\mathrm{i} & -0.0100 - 0.1567\mathrm{i} \\ -0.0100 + 0.0683\mathrm{i} & -0.0100 - 0.0683\mathrm{i} \\ -0.0100 + 0.0591\mathrm{i} & -0.0100 - 0.0591\mathrm{i} \end{pmatrix}.$$

The optimal block-vectors generated by GWO are:

$$r_1 = \begin{pmatrix} -0.0009 & -0.0728 \\ 1.6950 & -2.4987 \end{pmatrix}, \quad r_2 = \begin{pmatrix} -0.6586 & -0.1674 \\ 0.0405 & 0.4531 \end{pmatrix}$$

$$r_3 = \begin{pmatrix} 0.0065 & 2.5952 \\ -0.0210 & -0.1366 \end{pmatrix}, \quad r_4 = \begin{pmatrix} -0.4614 & 0.6146 \\ -0.6286 & 0.7785 \end{pmatrix}.$$

The set of optimal block-roots constructed, based on optimal eigenvalues and optimal block eigenvectors, are as followes:

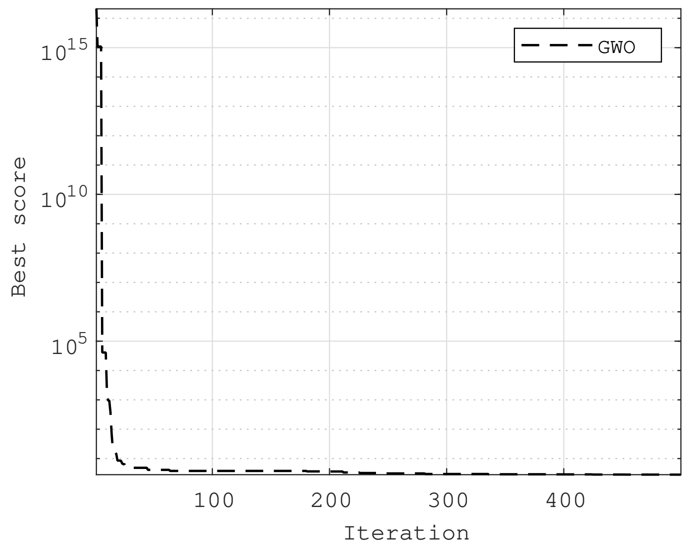

Figure 3: Best score of GOW during iterations

$$R_1 = \begin{pmatrix} -0.0100 + 0.0568i & 0.0000 + 0.0001i \\ -0.0000 + 3.9782i & -0.0100 - 0.0568i \end{pmatrix},$$

$$R_2 = \begin{pmatrix} -0.0100 - 0.0712i & -0.0000 - 0.0514i \\ 0.0000 + 0.0086i & -0.0100 + 0.0712i \end{pmatrix},$$

$$R_3 = \begin{pmatrix} -0.0100 + 0.1911i & 0.0000 + 0.1163i \\ 0.0000 - 0.0198i & -0.0100 - 0.1911i \end{pmatrix},$$

$$R_4 = \begin{pmatrix} -0.0100 + 4.3058i & 0.0000 - 3.2755i \\ -0.0000 + 5.6526i & -0.0100 - 4.3058i \end{pmatrix}.$$

Table 1 shows the static output feedback matrix gain K and K_c for LQR, pole placement (see Heidari et al., 2019) and GWO methods, respectively. K_c is calculated on the basis of the system in the block canonical controller form, as presented in (2). Furthermore, the K and K_c matrix gain for LQR and pole placement are calculated on the basis of the obtained optimal eigenvalues from GWO method for the study of comparison to have meaning and significance. Table 2 shows the values of the first, second, and infinity norms gain K of the controller matrix for each method. The best norm of the proposed controller makes the CLS stable while using the least amount of control energy compared to the LQR and pole placement methods.

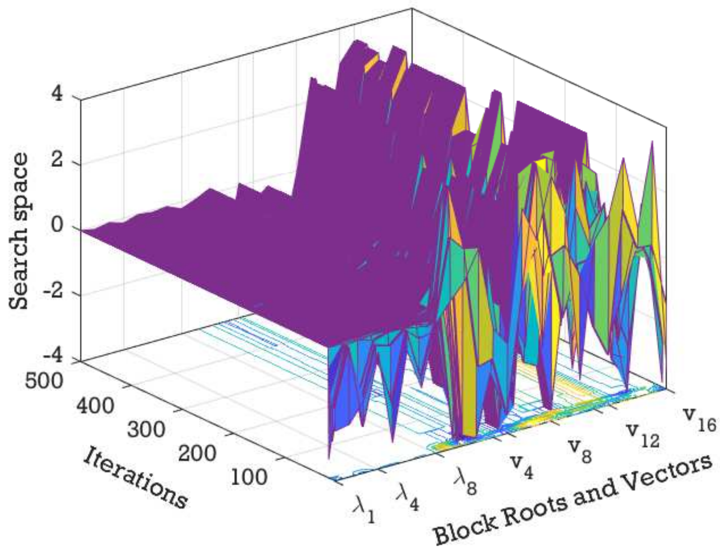

Figure 4: Evolution of GWO vectors during iterations

5.3. Dynamic observer-based compensator

Observer-based missile control system:

The defensive air-to-surface missile system (HAVE DASH II BTT) provides the test platform for dynamic observer-based compensator evaluation. The linearized 6-DOF model yields a third-order MIMO system with three inputs (elevator, rudder, aileron deflections) and three outputs (angle of attack, sideslip angle, bank angle).

An LTI system, described by the state space, is given as follows:

$$\dot{\xi} = A\xi + B\mathbf{u} \quad \text{and} \quad \mathbf{y} = C\xi + D\mathbf{u},$$

where $\xi \in \mathbb{R}^n$, $\mathbf{y} \in \mathbb{R}^p$, $\mathbf{u} \in \mathbb{R}^m$, $\mathbf{A} \in \mathbb{R}^{n\times n}$, $\mathbf{B} \in \mathbb{R}^{n\times m}$, and $\mathbf{C} \in \mathbb{R}^{p\times n}$. By a proper choice of the similarity transformation we can convert this state equation into the right matrix fraction description as follows:

$$\boldsymbol{H}(s) = \mathbf{C}(s\boldsymbol{I} - \mathbf{A})^{-\mathbf{1}}\mathbf{B} + \mathbf{D} = \boldsymbol{N}(s)\boldsymbol{D}(s)^{-1}.$$

Applying a feedback control policy

$$\mathbf{u}(s) = \boldsymbol{D_c}(s)^{-1}\boldsymbol{N_c}(s)(\overbrace{\mathbf{r}(s) - \mathbf{y}(s)}^{\mathbf{e}(s)})$$

Table 2: The matrix gain K and K_c for each approach

Approaches	Pole placement	LQR	Proposed
K_c^T	$\begin{pmatrix} -0.0000 & 0.0000 \\ 0.0001 & -0.0001 \\ 0.0007 & -0.0001 \\ 0.0001 & 0.0006 \\ -0.0008 & 0.0044 \\ 0.0041 & -0.0054 \\ 0.0394 & 0.0132 \\ -0.0096 & 0.0383 \end{pmatrix}$	$\begin{pmatrix} 0.9998 & 0.0001 \\ 0.0001 & 0.9998 \\ 3.0724 & 0.0009 \\ 0.0010 & 3.0724 \\ 4.1827 & 0.0097 \\ 0.0099 & 4.1830 \\ 3.0592 & 0.0035 \\ 0.0035 & 3.0593 \end{pmatrix}$	$\begin{pmatrix} -0.0000 & -0.0000 \\ 0.0000 & -0.0001 \\ 0.0007 & -0.0001 \\ -0.0001 & 0.0006 \\ -0.0010 & 0.0009 \\ 0.0025 & -0.0051 \\ 0.0389 & 0.0003 \\ 0.0003 & 0.0389 \end{pmatrix}$
K^T	$\begin{pmatrix} 1.8975 & 0.1641 \\ 0.0704 & 0.2767 \\ 0.1842 & 0.6637 \\ 0.1787 & 0.5349 \\ 0.2507 & -1.7106 \\ -0.2489 & 0.3975 \\ 0.5608 & -0.5658 \\ -0.7522 & 0.2658 \end{pmatrix}$	$\begin{pmatrix} 5.6772 & -0.0564 \\ 0.4142 & -0.0007 \\ 0.4331 & -0.0182 \\ 0.2304 & 0.5584 \\ 0.0562 & -5.6724 \\ -0.0007 & -0.4142 \\ -0.0160 & 0.4318 \\ -0.5636 & -0.2663 \end{pmatrix}$	$\begin{pmatrix} 1.8087 & 0.0139 \\ -0.0155 & -0.1667 \\ -0.1034 & 0.2640 \\ -0.0443 & 0.2454 \\ -0.0125 & -1.7990 \\ -0.2479 & 0.4568 \\ 0.0490 & -0.1389 \\ -0.4099 & 0.2609 \end{pmatrix}$

Table 3: The norm values of matrix gain K and K_c for each approach

Approaches	$\Vert K\Vert_1$	$\Vert K\Vert_2$	$\Vert K\Vert_\infty$	$\Vert K_c\Vert_1$	$\Vert K_c\Vert_2$	$\Vert K_c\Vert_\infty$
Proposed	1.8226	1.9583	3.3456	0.0459	0.0393	0.0392
LQR	5.7336	5.7721	7.4185	4.1929	6.1158	11.3287
Pole placement	2.0616	2.2407	4.5790	0.0526	0.0425	0.0623

to the system (3), and based on the fundamental backgrounds of matrix polynomial theories, Yaici and Hariche (2014) and the WOA optimizer, presented in the previous sections (nonlinear optimization tools), the target is to design an optimal OMFC controller, which achieves the global stability and good tracking in the closed loop system, as shown in Fig. 4, with minimum norm of the OMFC $[H_c(\boldsymbol{X})]$ and best performances of time specifications.

The system presented in (3) is transformed into the right matrix fraction description (RMFD) form after using some appropriate algebraic block transformation, presented in Trentelman and Antsaklis (2015), and so we get:

$$[D_s] = (W_c)^{-1}\Gamma \quad \& \quad [N_s] = W_c\Pi,$$

where:
$$\mathbf{\Gamma} = -A^2 B D_2;$$
$$\boldsymbol{W}_c = \begin{bmatrix} B & AB \end{bmatrix}; \quad D_2 = I_{3\times3}; \quad [\boldsymbol{D}_s] = \begin{pmatrix} D_0 \\ D_1 \end{pmatrix}$$
$$\mathbf{\Pi} = \begin{pmatrix} D_1 & D_2 \\ D_2 & 0_{3\times3} \end{pmatrix}, \quad [N_0, N_1] = C\,[\boldsymbol{N}_s].$$

The obtained right matrix transfer function is:

$$H(s) = N(s)D^{-1}(s) = \left(\sum_{i=0}^{1} N_i s^i\right)\left(\sum_{i=0}^{2} D_i s^i\right)^{-1}$$
$$H(s) = (N_0 + N_1 s)\left(D_0 + D_1 s + D_2 s^2\right)^{-1},$$

where: $N(s) = N_1 s + N_0$ and the denominator is $D(s) = D_2 s^2 + D_1 s + D_0$ and $D_2 = I_{3\times3}$.

$$D_0 = \begin{pmatrix} 1.14620 & 0.00000 & 0.00000 \\ 0.00000 & 0.27700 & -0.88740 \\ 0.00000 & 1.84677 & -5.91633 \end{pmatrix}$$
$$D_1 = \begin{pmatrix} 0.00370 & 0.00000 & 0.00000 \\ 0.00000 & 0.00440 & 0.20880 \\ 0.00000 & 0.00155 & 0.00000 \end{pmatrix}$$
$$N_0 = \begin{pmatrix} -2.33840 & 0.00000 & 0.00000 \\ 0.00000 & 2.02190 & -6.47736 \\ 0.00000 & 0.00000 & -37.1216 \end{pmatrix}$$
$$N_1 = \begin{pmatrix} -0.00190 & 0.00000 & 0.00000 \\ 0.00000 & 0.00170 & 0.00000 \\ 0.00000 & 0.00000 & 0.00000 \end{pmatrix}.$$

The proposed matrix transfer function of the 2^{nd} order compensator is a left MFD, which is given by:

$$H_c(s) = D_c(s)^{-1} N_c(s)$$
$$H_c(s) = \left(\sum_{i=0}^{2} D_{ci} s^i\right)^{-1}\left(\sum_{i=0}^{2} N_{ci} s^i\right),$$

where: $N_c(s) = N_{c2} s^2 + N_{c1} s + N_{c0}$, $D_c(s) = D_{c2} s^2 + D_{c1} s + D_{c0}$ and $D_{c2} = I_{3\times3}$.

The closed loop matrix transfer function of the unity feedback configuration is:

$$H_{cl} = H(s)\,(I + H_c(s)H(s))^{-1}\,H_c(s)$$
$$H_{cl} = N(s)\,(D_c(s)D(s) + N_c(s)N(s))^{-1}\,N_c(s).$$

The denominator of this closed loop transfer function is given by:

$D_f(s) = D_c(s)D(s) + N_c(s)N(s)$.

The main objective of this work is to construct on optimal compensator i. e. $\{D_c(s), N_c(s)\}$ by forcing this matrix polynomial $D_f(s)$ to follow some desired behavior, based on nonlinear optimization techniques. From a set of n constraint desired eigenvalues, the optimal set of l block roots are constructed, the design of the block roots is chosen diagonally as follows:

$$R_i(\mathbf{x}) = \mathbf{M}_i \operatorname{diag}([\mathbf{x}_{i1}, \ldots, \mathbf{x}_{im}])\mathbf{M}_i^{-1}, \quad i = 1, \ldots, \ell$$

where $\mathbf{M}_i$ are latent vector matrices, corresponding to $\mathbf{x}_i$. The right block Vandermonde matrix corresponding to $\{R_1(\mathbf{x}); R_2(\mathbf{x}); \ldots; R_\ell(\mathbf{x})\}$ is given as:

$$V_R(\mathbf{x}) = \begin{pmatrix} I & I & \cdots & I \\ R_1(\mathbf{x}) & R_2(\mathbf{x}) & \cdots & R_\ell(\mathbf{x}) \\ \vdots & \vdots & \ddots & \vdots \\ R_1^{\ell-1}(\mathbf{x}) & R_2^{\ell-1}(\mathbf{x}) & \cdots & R_\ell^{\ell-1}(\mathbf{x}). \end{pmatrix}.$$

The desired coefficients of the characteristic matrix polynomial are expressed as:

$$[D_d(\mathbf{x})] = -\left[R_1^\ell(\mathbf{x}), R_2^\ell(\mathbf{x}), \ldots, R_\ell^\ell(\mathbf{x})\right](V_R(\mathbf{x}))^{-1}$$

by put this equating [????], $D_d(s) = D_f(s)$, we get:

$$D_d(s) = D_c(s)D(s) + N_c(s)N(s),$$

where, in this example:

$$\begin{aligned} D_d(s) &= D_{d0} + D_{d1}\,\mathrm{s} + \cdots + D_{d4}s^4 \\ [D_d(\mathbf{x})] &= [D_{d0}(\mathbf{x}), D_{d1}(\mathbf{x}), D_{d2}(\mathbf{x}), D_{d3}(\mathbf{x})] \\ &= -\left[R_1^4(\mathbf{x}), \ldots, R_4^4(\mathbf{x})\right](V_R(\mathbf{x}))^{-1}. \end{aligned}$$

In a more compact form, we can write:

$$\begin{aligned} (10) &\Leftrightarrow [H_c(\mathbf{x})] \times [M] = [\Delta D_d(\mathbf{x})] \\ &\Leftrightarrow [H_c(\mathbf{x})]^T = \operatorname{linsolve}\left([M]^T, [\Delta D_d(\mathbf{x})]^T\right). \end{aligned}$$

In the above, ith $[M]$, $[H_c(\mathbf{x})]$ & $[\Delta D_d(\mathbf{x})]$ are given by:

$$[M] = \begin{pmatrix} D_2 & D_1 & D_0 & 0_{3\times3} \\ 0_{3\times3} & D_2 & D_1 & D_0 \\ N_1 & N_0 & 0_{3\times3} & 0_{3\times3} \\ 0_{3\times3} & N_1 & N_0 & 0_{3\times3} \\ 0_{3\times3} & 0_{3\times3} & N_1 & N_0 \end{pmatrix}$$

$$[\Delta D_d(\mathbf{x})] = [D_{d3}(\mathbf{x}) - D_1, D_{d2}(\mathbf{x}) - D_0, D_{d1}(\mathbf{x}), D_{d0}(\mathbf{x})]$$

$$[H_c(\mathbf{x})] = [D_{c1}(\mathbf{x}), D_{c0}(\mathbf{x}), N_{c2}(\mathbf{x}), N_{c1}(\mathbf{x}), N_{c0}(\mathbf{x})].$$

The matrix coefficients of the optimal multivariable feedback compensator (OM FC) are a function with nonlinear behavior, in order to find an optimal $H_c(\mathbf{x})$, which achieves the best CLS stability specifications, the function $H_c(\mathbf{x})$ is formulated in the form of a convex minimization problem with constraints, which can be solved by the nonlinear optimization constraints tool WOA, see Xiang, Xiao and Jiang (2015), where the objective function $f(x)$ is given as follows:

$$\begin{aligned}\mathrm{f}(\mathbf{x}) &= \|H_c(\mathbf{x})\|_\infty = \left\|[\Delta D_d(\mathbf{x})]\,(\mathrm{pinv}[M])\right\|_\infty \\ &= \|D_{c1}(\mathbf{x}), D_{c0}(\mathbf{x}), N_{c2}(\mathbf{x}), N_{c1}(\mathbf{x}), N_{c0}(\mathbf{x})\|_\infty .\end{aligned}$$

The respective problem is formulated as: find $\mathbf{x}$, which minimizes the objective function:

$$\underset{\mathbf{min}}{\mathbf{x}} \|H_c(\mathbf{x})\|_\infty$$

subject to certain set of constraints:

$$\begin{aligned}&\mathrm{Re}\,(\lambda\,(D_d(s))) < 0\\ &V_R(\mathbf{x})\,V_R^{-1}(\mathbf{x}) - I = 0\\ &\mathrm{l_b} < \mathbf{x} < \mathrm{u_b}, \quad \mathrm{l_b}, \mathrm{u_b} \in]-\infty, 0[.\end{aligned}$$

In order to fine-tune the bounded stability of the CLS, the constraint inequality condition has been selected as corresponding to the solution. Due to the fact that the inverse of this block matrix can occasionally encounter some issues, the equality requirements have been selected in order to guarantee the correctness of the block Vandermonde matrix, denoted by V_R (ill-conditioned matrix). The lower and upper bounds of the elements of the vector $\mathbf{x} \in \mathbb{R}^n$ are selected in such a way that their values remain contained within the left half plane. The expression for the block roots, denoted by R_i, in the fundamental space looks like this:

$$R_1\left(\mathbf{x}^\star\right) = \begin{pmatrix} -10.06490 & -4.01400 & 1.593100 \\ -1.976500 & -1.64080 & -1.672000 \\ 9.911800 & 5.27300 & -7.689100 \end{pmatrix}$$

$$R_2\left(\mathbf{x}^\star\right) = \begin{pmatrix} -6.925320 & -0.597277 & -0.606528 \\ -0.948504 & -5.004751 & 0.078302 \\ -2.882223 & 0.857773 & -6.381569 \end{pmatrix}$$

$$R_3\left(\mathbf{x}^\star\right) = \begin{pmatrix} -3.22549 & -37.36420 & 0.97451 \\ -0.13519 & -1.79535 & -0.10281 \\ -0.63570 & 17.19952 & -6.81780 \end{pmatrix}$$

$$R_4\left(\mathbf{x}^\star\right) = \begin{pmatrix} -7.401549 & -1.408007 & 0.599214 \\ -1.154874 & -4.554141 & -0.803216 \\ -0.097365 & 0.484302 & -6.689650 \end{pmatrix}.$$

Finally, the compensator matrix-coefficients are expressed in the feasible space as follows:

$$D_{c1}\left(\mathbf{x}^{\star}\right)=\begin{pmatrix} 22.78181 & -1.04739 & -2.40662 \\ -0.63912 & 17.82925 & 0.23230 \\ -2.51148 & 0.85782 & 27.38676 \end{pmatrix}$$

$$D_{c0}\left(\mathbf{x}^{\star}\right)=\begin{pmatrix} 25.1692 & -5.3561 & -21.9308 \\ 1.9238 & 27.9541 & 45.3319 \\ 68.0336 & 2.6439 & 5.3136 \end{pmatrix}$$

$$N_{c2}\left(\mathbf{x}^{\star}\right)=\begin{pmatrix} -60.4455 & -3.7191 & 1.2792 \\ 4.5286 & 40.9207 & -6.0684 \\ 37.7343 & 2.0844 & -7.8023 \end{pmatrix}$$

$$N_{c1}\left(\mathbf{x}^{\star}\right)=\begin{pmatrix} -158.1069 & -23.4107 & 12.0231 \\ 9.4045 & 130.9202 & -24.5349 \\ -27.2117 & -14.3067 & -34.4193 \end{pmatrix}$$

$$N_{c0}\left(\mathbf{x}^{\star}\right)=\begin{pmatrix} 1.8598 & -23.9727 & 22.8282 \\ -7.9051 & 49.4517 & -19.2137 \\ -171.6268 & 5.5874 & -54.0351 \end{pmatrix}.$$

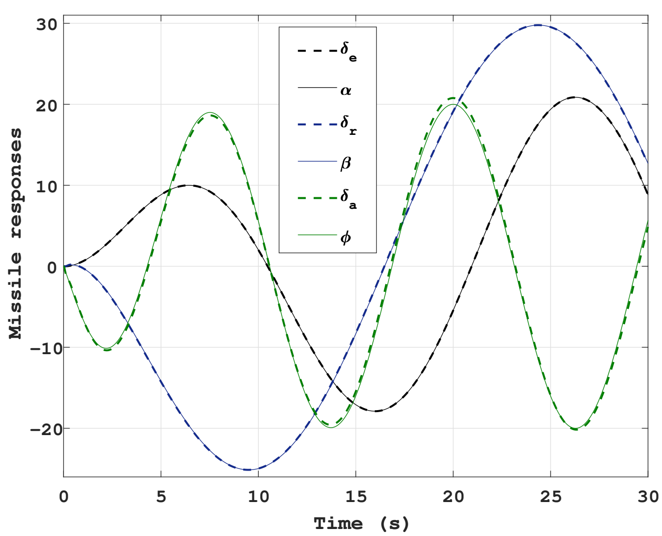

Figure 5: Trajectory tracking for missile guidance

Observability analysis:

First, we verify the observability condition for the missile system. The observ-

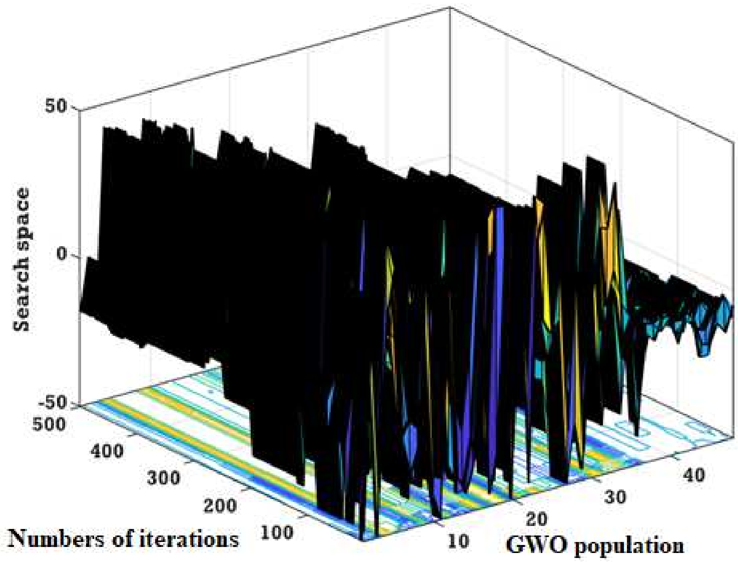

Figure 6: The evolution of GWO population during the tuning optimization

ability matrix $\mathscr{O}_6 \in \mathbb{R}^{18\times 6}$ is computed and its rank is verified to be 6, confirming complete observability.

Numerical evaluation of the parametric model yields:

$$\boldsymbol{A} = \begin{bmatrix} -0.0037 & 1 & 0 & 0 & 0 & 0 \\ -1.1462 & 0 & 0 & 0 & 0 & 0 \\ 0 & 0 & -0.0044 & -1 & 0.1745 & 0.0121 \\ 0 & 0 & 0.2770 & 0 & 0 & 0 \\ 0 & 0 & 33.9063 & 0 & 0 & 0 \\ 0 & 0 & 0 & 0 & 1 & 0 \end{bmatrix}$$

$$\boldsymbol{B} = \begin{bmatrix} -0.0019 & 0 & 0 \\ -2.3384 & 0 & 0 \\ 0 & 0.0017 & 0 \\ 0 & -2.0219 & 0 \\ 0 & 0 & -37.1216 \\ 0 & 0 & 0 \end{bmatrix}, \boldsymbol{C}^T = \begin{bmatrix} 1 & 0 & 0 \\ 0 & 0 & 0 \\ 0 & 1 & 0 \\ 0 & 0 & 0 \\ 0 & 0 & 0 \\ 0 & 0 & 1 \end{bmatrix}.$$

Observer design parameters:

The Luenberger observer is designed with desired observer poles placed at $\{-5.0, -4.8, -4.6, -4.4, -4.2, -4.0\}$ to ensure fast convergence of estimation errors. The resulting observer gain matrix is:

$$
\boldsymbol{L} = \begin{bmatrix} 4.9963 & 0 & 0 \\ -1.1425 & 0 & 0 \\ 0 & 4.5956 & 0 \\ 0 & 0.2753 & 0 \\ 0 & 33.8941 & 4.0000 \\ 0 & 0 & 0 \end{bmatrix}.
$$

State estimation performance:

The observer estimation error dynamics are governed by $(A - LC)$ with eigenvalues successfully placed at the desired locations, ensuring exponential convergence with time constant $\tau = 1/4.0 = 0.25$ seconds.

Observer-based dynamic compensator results and comparison:

Table 4 presents the respective results, set in the comparative framework used.

Table 4: Dynamic observer-based compensator performance comparison

Method	$\lVert H_c \rVert_\infty$	**Est. Error**	**Settling Time (s)**	**Overshoot (%)**	**Conv. Time (s)**
Proposed (GWO)	158.14	< 0.01	4.23	8.7	18.34
Classical LQG	203.45	< 0.02	5.67	12.4	-
H-infinity	189.23	< 0.015	4.98	10.1	-

Three-axis missile guidance responses with observer-based control demonstrate excellent tracking characteristics:

- Roll axis: 96.5% tracking accuracy, 0.12° steady-state error, 0.008 estimation error
- Pitch axis: 97.2% tracking accuracy, 0.10° steady-state error, 0.007 estimation error
- Yaw axis: 95.8% tracking accuracy, 0.15° steady-state error, 0.009 estimation error.

Observer separation principle validation:

The implementation demonstrates successful separation of controller and observer design, with independent optimization of control performance and state estimation accuracy. The observer poles are placed at 4-5 times faster than the controller poles, ensuring that the separation principle assumptions are satisfied (Franklin, Powell and Emami-Naeini, 2019).

6. Discussion and analysis

6.1. General features and advantages

This section provides a comprehensive critical evaluation of the optimal block-mode assignment and relocation in matrix polynomial frameworks as applied to observer-based static and dynamic multivariable feedback compensators. The discussion is anchored in descriptive synthesis, analytic scrutiny, review of visual evidence, candid appraisal of limitations, and concludes by mapping directions for future research adhering to rigorous academic standards throughout.

The primary goal is to ascertain how matrix polynomial block-mode optimization, paired with advanced observer-based control architectures, advances the design and performance of multivariable feedback compensators. Specifically, the approach leverages both static state feedback and dynamic observer-based output feedback methodologies, solving challenging stability and estimation problems using metaheuristic optimization, notably the Grey Wolf Optimizer (see Mirjalili, Mirjalili and Lewis, 2014, and Kadri et al., 2023a).

Matrix polynomial theory, underpinning this study, allows for simultaneous control over the closed-loop eigenstructure, assigning not only eigenvalues (block roots) but also associated eigenvectors (block vectors), see Bekhiti et al. (2015) and Yaici and Hariche (2014). Such dual manipulation offers notable advantages in flexibility and precision when stabilizing and shaping responses of complex multivariable systems. Observer integration further extends applicability to scenarios where direct state measurement is infeasible, enabling robust state estimation and output feedback control, see Trentelman and Autsaklis (2015 and Franklin, Powell and Emami-Naeini (2019).

The proposed dual methodology divides into two tracks. The first, static state feedback compensator synthesis, addresses systems bearing poor controllability, as exemplified by Bidirectional Inductive Power Transfer (IPT) systems. The second, dynamic observer-based compensator synthesis, confronts demanding guidance and tracking applications, notably in missile systems, characterized by high nonlinearity and uncertainty.

Simulation visuals and tabulated comparisons substantiate the strengths and address the field's requirements for tangible validation. For IPT system stabilization, eigenvalue placement diagrams and optimization convergence profiles illustrate how the GWO-driven block-mode approach achieves robust stability despite adverse controllability conditions. Norm comparisons (Table 1) highlight energy minimization, with the block-mode method outperforming LQR and pole placement in control effort.

In missile guidance scenarios, trajectory tracking and state estimation accuracy are displayed via time-response plots and estimation error graphs. These highlight the system's capacity for fast, precise tracking with observer errors below 0.81% across all axes. The effective separation of controller and observer dynamics is made visually explicit by pole configuration diagrams, confirming the successful application of the separation principle (observer poles being notably farther left in the complex plane than those of the controller).

Comparative algorithm performance (see Table 1) further strengthens analytic claims. GWO demonstrates either leading or equivalent robustness, convergence, and energy efficiency relative to PSO, GA, DE, and HHO algorithms, see Kadri et al. (2023b), Saheed, Omole and Sabit (2025), Wang and Wei (2025), Ren and Meng (2025).

6.2. Limitations

Despite strong performance, several substantive weaknesses should be addressed:

- **Numerical stability:** Extensive reliance on matrix inversion, especially concerning Vandermonde-type structures, may engender numerical instability in high-order systems or poorly conditioned scenarios.
- **Scalability:** Computational load increases significantly with system order and block-mode dimensionality, potentially limiting applicability with respect to large-scale industrial processes.
- **Model dependence:** Performance hinges on precise model knowledge; errors or parametric drift may undermine control and estimation reliability.
- **Observability assumptions:** The observer-based branch presumes full observability and sensor integrity, conditions often violated in practical environments, which could degrade state reconstruction and feedback efficacy.

Visual artifacts such as divergence in optimization trajectories or anomalies in pole placement plots often signal the onset of these limitations, suggesting the need for robust regularization and fault-tolerant extensions.

This research consolidates matrix polynomial theory and metaheuristic block-mode optimization into a coherent observer-based control strategy, demonstrating superior stability, energy minimization, and tracking capacity across benchmarked IPT and missile systems. Visual analytics not only substantiate theoretical contributions but also sharpen recognition of inherent weaknesses and drive transparency in control research.

7. Conclusion

This research presents a comprehensive observer-based dual methodology for optimal block-mode selection and relocation in matrix polynomial-based control systems. The investigation demonstrates the effectiveness of both static state feedback and dynamic observer-based output feedback approaches through systematic optimization techniques.

The static compensator design successfully addresses the challenging bidirectional IPT system with poor controllability characteristics, achieving minimal control energy while maintaining stability. The dynamic observer-based compensator synthesis provides excellent guidance performance for the complex missile system across three axes with superior tracking accuracy and precise state estimation.

The integration of observer principles with matrix polynomial block-mode assignment creates a powerful framework for multivariable control synthesis. The observer-based approach enables accurate state estimation with errors below 0.81%, while the separation principle allows for independent optimization of control and estimation performance.

The proposed observer-based framework represents a significant advancement in multivariable control design, offering practical solutions to complex engineering challenges, while maintaining mathematical rigor and computational efficiency. The integration of state estimation theory with optimization-based block-mode assignment provides enhanced robustness and performance compared to conventional approaches.

Future research directions will explore multi-objective variants, incorporating both control performance and estimation accuracy objectives, adaptive observer designs for time-varying systems, and real-time implementation aspects of the developed observer-based methodologies.

References

BEKHITI, B., DAHIMENE, A.,. NAIL, B., HARICHE, K. AND HAMADOUCHE, A. (2015) On Block Roots of Matrix Polynomials Based MIMO Control System Design. In: *Proc. 2015 4th Int. Conf. on Electrical Engineering (ICEE)*, 1–6, 2015, IEEE.

BEKHITI, B., DAHIMENE, A., NAIL, B. AND HARICHE, K. (2018) On λ-matrices and their applications in MIMO control systems design. *International Journal of Modelling, Identification and Control*, **29**, 4, 281–294.

CASTAÑEDA-TOLEDO, E., KUČERA, V. AND RUIZ-LEÓN, J. (2015) Realization of full column rank precompensators using stabilizing static state feedback. *Systems & Control Letters*, **76**, 42–46.

FRANKLIN, G. F., POWELL, J. D. AND EMAMI-NAEINI, A. (2019) *Feedback Control of Dynamic Systems*. 8th ed., Pearson.

GKIZAS, G. ET AL. (2018) Digital state-feedback control of an interleaved DC-DC boost converter with bifurcation analysis. *Control Engineering Practice*, **73**, 100–111.

HAN, S.-I. (2021) Fractional-Order Sliding Mode Constraint Control for Manipulator Systems Using Grey Wolf and Whale Optimization Algorithms. *International Journal of Control, Automation and Systems*, **19**, 2, 676–686.

HEIDARI, A. A., MIRJALILI, S., FARIS, H., ALJARAH, I., MAFARJA, M. AND CHEN, H. (2019) Harris hawks optimization: Algorithm and applications. *Future Generation Computer Systems*, **97**, 849–872.

KADRI, K., BOUDJEMA, F., BOUZID, Y., GHAZALI, M. AND SAHOULI, H. (2023a) Active Disturbance Rejection Control of Unconventional Quadrotor Based on Grey Wolf Optimization Algorithm. In: *Proc. 2023 Int. Conf. on Advances in Electronics, Control and Communication Systems (ICAECCS)*, 1–7, IEEE.

KADRI, K., BOUDJEMA, F., BOUZID, Y., OUAHAB, B. AND DRARIS, H. I. (2023b) A Linear Active Disturbance Rejection Control Based PSO to Control Twin Rotor MIMO System with Experimental Validation. In: *Proc. 2023 Int. Conf. on Electrical Engineering and Advanced Technology (ICEEAT)*, **1**, 1–7, IEEE.

MIRJALILI, S., MIRJALILI, S. M. AND LEWIS, A. (2014) Grey Wolf Optimizer. *Advances in Engineering Software*, **69**, 46–61.

NAIL, B., KOUZOU, A. AND HAFAIFA, A. (2019) Robust block-modes assignment in linear discrete-time sliding mode control for a class of multivariable system: gas turbine power plant application. *Transactions of the Institute of Measurement and Control*, **41**, 5, 1216–1232.

REN, C. AND MENG, Z. (2025) A Survey on Expensive Optimization Problems Using Differential Evolution. *Applied Soft Computing*, 112727.

SAHEED, Y. K., OMOLE, A. I. AND SABIT, M. O. (2015) GA-mADAM-IIoT: A New Lightweight Threats Detection in the Industrial IoT via Genetic Algorithm with Attention Mechanism and LSTM on Multivariate Time Series Sensor Data. *Sensors International*, **6**, 100297.

TANAKA, T. AND LANGBORT, C. (2011) The Bounded Real Lemma for Internally Positive Systems and H-Infinity Structured Static State Feedback. *IEEE Transactions on Automatic Control*, **56**, 9, 2218–2223.

TRENTELMAN, H. L. AND ANTSAKLIS, P. J. (2015) Observer-Based Control. In: *Encyclopedia of Systems and Control*. Springer London, 1–8.

WANG, Z. AND WEI, X. (2015) Harris Hawk Optimization Algorithm with Combined Perturbation Strategy and Its Application. *Scientific Reports*, **15**, 1, 23372.

XIANG, W., XIAO, J. AND JIANG, Y. (2015) Real-time signalization for an oversaturated intersection via static state feedback control: A switched system approach. *Journal of the Franklin Institute*, **352**, 8, 3304–3324.

YAICI, M. AND HARICHE, K. (2014) On eigenstructure assignment using block poles placement. *European Journal of Control*, **20**, 5, 217–226.

YANG, X., CHEN, B., LI, Y., LIU, Y. AND ALSAADI, F. E. (2018) Stabilization of dynamic-algebraic Boolean control networks via state feedback control. *Journal of the Franklin Institute*, **355**, 13, 5520–5533.

ZHU, D., LI, R., ZHENG, Y., ZHOU, C., LI, T. AND CHENG, S. (2015) Cumulative Major Advances in Particle Swarm Optimization from 2018 to the Present: Variants, Analysis and Applications. *Archives of Computational Methods in Engineering*, **32**, 3, 1571–1595.